



Neutron irradiation of polycrystalline yttrium aluminate garnet, magnesium aluminate spinel and α -alumina

E.A.C. Neeft^{a,*}, R.J.M. Konings^{a,1}, K. Bakker^a, J.G. Boshoven^a, H. Hein^a,
R.P.C. Schram^a, A. van Veen^b, R. Conrad^c

^a Nuclear Research and Consultancy Group, P.O. Box 25, NL-1755 ZG Petten, The Netherlands

^b Interfaculty Reactor Institute, Delft University of Technology, Mekelweg 15, NL-2629 JB Delft, The Netherlands

^c European Commission, Joint Research Centre, Institute for Advanced Materials, P.O. Box 2, NL-1755 ZG Petten, The Netherlands

Abstract

Polycrystalline pellets of yttrium aluminate garnet ($Y_3Al_5O_{12}$), magnesium aluminate spinel ($MgAl_2O_4$) and α -alumina (α - Al_2O_3) have been irradiated in the high flux reactor (HFR) at Petten to a neutron fluence of $1.7 \times 10^{26} \text{ m}^{-2}$ ($E > 0.1 \text{ MeV}$) at a temperature of about 815 K. Volume changes smaller than 1% have been measured for $Y_3Al_5O_{12}$ and $MgAl_2O_4$. Transmission electron microscopy (TEM) results of $Y_3Al_5O_{12}$ show no difference between the unirradiated TEM samples and neutron-irradiated samples. For $MgAl_2O_4$, dislocation loops in some grains are found in the irradiated samples. TEM results of Al_2O_3 show a dense network of dislocation loops after neutron irradiation. The increase in volume is 4.2% for a neutron fluence of $1.7 \times 10^{26} \text{ m}^{-2}$. © 1999 Elsevier Science B.V. All rights reserved.

1. Introduction

Transmutation of actinides like americium and plutonium in a uranium free matrix is a promising fuel concept to reduce the radiotoxicity of high-level nuclear waste. The uranium free matrix suffers damage from neutrons, fission products, α -particles and recoil atoms. The damage from neutrons on the uranium free matrices yttrium aluminate garnet ($Y_3Al_5O_{12}$) and magnesium aluminate spinel ($MgAl_2O_4$) are discussed in this study. α -Alumina (α - Al_2O_3) is used as a reference material.

Polycrystalline pellets of these three materials are neutron irradiated in the high flux reactor (HFR) at Petten. The post-irradiation examination consists of dimensional measurements, as well as optical microscopy and transmission electron microscopy (TEM) investigations.

This research is a continuation of a previous neutron irradiation experiment at a temperature of 815 K. The neutron fluence (ϕ_n) in the previous experiment was $0.46 \times 10^{26} \text{ m}^{-2}$ ($E > 0.1 \text{ MeV}$) [1]. The same polycrystalline materials are neutron irradiated up to a neutron fluence (ϕ_n) of $1.7 \times 10^{26} \text{ m}^{-2}$ in the present study.

2. Experiments

2.1. Pre- and post-irradiation experimental methods

Powders of $Y_3Al_5O_{12}$ (Gimex) and Al_2O_3 (ALCO CT3000sg) are isostatically pressed into rods at a pressure of 200 MPa and presintered at 1273 K in air. Next, the rods are mechanically processed and cut into pellets. Finally, the pellets are sintered in air at 1873 K. All pellets have a white colour, except for Al_2O_3 which is slightly reddish. Spray dried powder of spinel (Baikowski, S28R) is uniaxially pressed into pellets at a pressure of 85 MPa and sintered in air at 1873 K for 10 h. The dimensions of the pellets are measured with a Mitutoyo micrometer with an accuracy of $\pm 0.005 \text{ mm}$.

The irradiated and unirradiated pellets are cut, embedded in Hysol, grazed with SiC-paper and polished

* Corresponding author. Fax: +31-224 563 608; e-mail: neeft@nrg-nl.com

¹ Present address: European Commission Joint Research Centre, Institute for Transuranium Elements, Postfach 2340, D-76125 Karlsruhe, Germany

with diamond paste for optical examination. Magnifications of 20 \times , 100 \times and 500 \times of $Y_3Al_2O_{12}$ and $MgAl_2O_4$ show very fine distributions of pores. Scanning electron microscopy (SEM) examinations show that the diameter of the pores varies from 0.2 to 2 μm for $MgAl_2O_4$ and from 0.2 to 3 μm for $Y_3Al_5O_{12}$. Fine pores and pore clusters with a size of about 80–100 μm are observed in pellets of Al_2O_3 . The highest magnification of this SEM is 1500 \times thus pores with a size of a few nanometers may be present but cannot be detected with this technique.

No open porosity in the sintered pellets could be determined using mercury porosimetry. The grain size, X-ray analysis, amount of impurities and theoretical density of the unirradiated pellets are reported by Konings et al. [1].

TEM samples have been prepared by crushing unirradiated and irradiated pellets and sieving very small particles with a carbon-coated Cu grid (Pfeiffer) from a twice distilled water suspension. The resolving power of the TEM (Philips 301) microscope with an accelerating voltage of 100 kV is about 1 nm.

The unirradiated pellets are examined to confirm that the observed microstructure in the irradiated pellets are not induced by the preparation of the TEM sample. No voids or dislocation loops are present in the unirradiated materials.

2.2. Irradiation

The pellets are encapsulated in a Zircaloy-4 tube. The pellets are kept in position by a stainless steel spring. The Zircaloy capsules are filled with helium gas (1 bar at room temperature) and are welded by laser. The samples are irradiated in central in-core positions of the HFR. The gamma heating rate of the samples and the aluminium sample holders is about 10.9 W g⁻¹. Temperature control is done by the gas mixture technique and the sample holders are measured to be 713 K during the neutron irradiation. There are three media between the pellets and the aluminium sample holder: first, the He-filled gap between the pellets and the Zircaloy tube, next, the Zircaloy tube and finally, the He-filled gap between the Zircaloy tube and the aluminium sample holder. The temperature of the pellets is calculated to be 815 K when

Table 1
Irradiation conditions of the pellets

| Power days | 101.1 | 404.4 |
|----------------------------------|-----------------------|-----------------------|
| ϕ_n/m^{-2} ($E > 0.1$ MeV) | 0.46×10^{26} | 1.7×10^{26} |
| ϕ_n/m^{-2} ($E > 1.0$ MeV) | 0.22×10^{26} | 0.82×10^{26} |
| γ -dose (Gy) | 95×10^9 | 381×10^9 |
| Temperature (K) | 815 | 815 |

the thermal conductivities of Zircaloy and of helium are taken into account. Quantitative data of the irradiation conditions are described in Table 1.

3. Results

Table 2 shows the size of unirradiated pellets and the volume changes of these pellets after neutron irradiation in the present study. Optical photographs with magnifications 20 \times , 100 \times and 500 \times do not show differences between the unirradiated and the irradiated pellets for both neutron fluences, except for spinel. One pellet is examined for each ϕ_n . For both neutron fluences, spinel shows one radial crack from the core to the rim. Two additional pellets for each ϕ_n have been investigated to ensure that this feature is not incidental. Again, one radial crack from core to the rim is observed in each of the two other pellets.

For $Y_3Al_5O_{12}$, no difference between the unirradiated TEM samples and the irradiated samples is observed for a ϕ_n of 1.7×10^{26} m⁻².

$MgAl_2O_4$ shows almost no difference between the unirradiated TEM samples and irradiated samples for both neutron fluences. However, in some grains, separate dislocation loops (Fig. 1) are observed for a ϕ_n of 1.7×10^{26} m⁻².

TEM samples show a dense network of dislocation loops in the grains of Al_2O_3 for both neutron fluences which are not observed in unirradiated pellets. Fig. 2 shows a neutron-irradiated Al_2O_3 grain for a ϕ_n of 1.7×10^{26} m⁻². In neutron-irradiated pellets, very few grain boundaries are observed in the TEM samples. In unirradiated Al_2O_3 TEM samples, many grain boundaries are observed.

Table 2
Properties and results of the polycrystalline materials

| | Size of unirradiated pellets | | Number of pellets | $(100 \times \Delta V \bullet V^{-1})/\%$ | |
|-----------------|------------------------------|-------------|-------------------|---|--|
| | Diameter (mm) | Height (mm) | | ϕ_n (m ⁻²) 0.46×10^{26} | ϕ_n (m ⁻²) 1.7×10^{26} |
| $Y_3Al_5O_{12}$ | 9.0 | 10.2 | 5 | $+0.54 \pm 0.26$ | $+0.44 \pm 0.23$ |
| $MgAl_2O_4$ | 9.0 | 4.8–5.0 | 10 | -0.63 ± 0.78 | -0.40 ± 0.65 |
| Al_2O_3 | 9.1 | 10.0 | 5 | $+1.9 \pm 0.27$ | $+4.2 \pm 0.27$ |

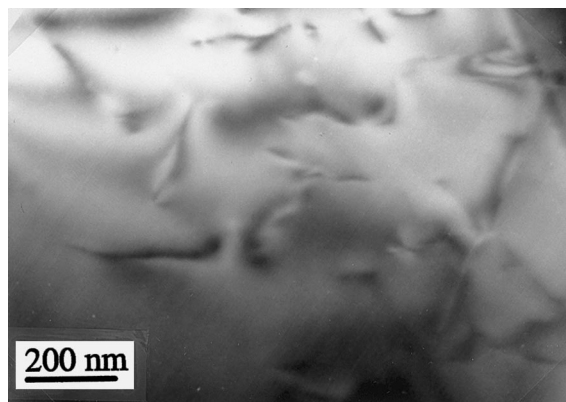


Fig. 1. TEM image of neutron-irradiated MgAl_2O_4 ($1.7 \times 10^{26} \text{ m}^{-2}$, 815 K) ($E > 0.1 \text{ MeV}$).



Fig. 2. TEM image of neutron-irradiated Al_2O_3 ($1.7 \times 10^{26} \text{ m}^{-2}$, 815 K) ($E > 0.1 \text{ MeV}$).

4. Discussion

The damage created by neutron irradiation is investigated for Al_2O_3 and MgAl_2O_4 at temperatures of 673–873 K and amounts to 1 displacement per atom (dpa) for a ϕ_n of 10^{25} m^{-2} ($E > 0.1 \text{ MeV}$) [2]. In this study, the amount of dpa for Al_2O_3 and MgAl_2O_4 is therefore estimated to be 4.6 dpa and 17 dpa for both neutron fluences, respectively. The present study describes neutron irradiation in a water-cooled reactor. Almost all neutron irradiation studies of polycrystalline Al_2O_3 and MgAl_2O_4 were performed in sodium-cooled reactors.

The neutron- and γ -spectra are different for these reactors; the damage rate (i.e. fast neutron flux) and radiation-induced mobility of interstitials and vacancies may therefore be different. There are no studies on the amount of displacements in $\text{Y}_3\text{Al}_5\text{O}_{12}$ caused by neutron irradiation, known to the authors.

4.1. Yttrium aluminate garnet

Fig. 3 shows the volume change of polycrystalline $\text{Y}_3\text{Al}_5\text{O}_{12}$ versus ϕ_n . The slight increase in volume in the study by Mitchell and Youngman [3] was attributed to the presence of the Al_2O_3 -phase on the grain boundaries which swelled with neutron irradiation. In the studies from Mitchell and Youngman [3], and from Hurley and Bunch [4], no X-ray analysis was shown before polycrystalline $\text{Y}_3\text{Al}_5\text{O}_{12}$ irradiation by neutron. These authors reported, however, the same neutron irradiation study of polycrystalline $\text{Y}_3\text{Al}_5\text{O}_{12}$ as reported in this work.

In the present study, X-ray analysis shows that only the phase $\text{Y}_3\text{Al}_5\text{O}_{12}$ [1] is present in the pellet. Also, no difference is observed between unirradiated TEM samples and neutron-irradiated samples; samples with a high density of dislocation loops are expected when an Al_2O_3 phase in $\text{Y}_3\text{Al}_5\text{O}_{12}$ is present. The irradiation temperature may also have an impact on the observed difference between the present study and the other work [3,4]. The slight increase in volume in the present study has probably another cause e.g. unresolvable displacement damage; point defects with a size of about 1 Å cannot be detected by TEM with a resolving power of 1 nm.

The observation of the absence of defect clusters in the grains after neutron irradiation of $\text{Y}_3\text{Al}_5\text{O}_{12}$ by TEM in the present study, was also reported after neutron irradiation of single crystals of $\text{Y}_3\text{Al}_5\text{O}_{12}$ at temperatures of 925 and 1015 K [5] and polycrystalline

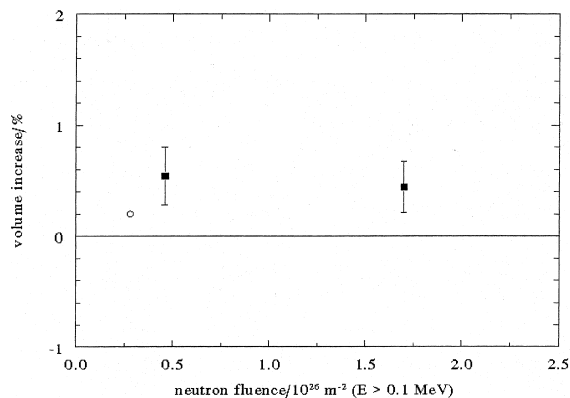


Fig. 3. The swelling of polycrystalline $\text{Y}_3\text{Al}_5\text{O}_{12}$ as a function of ϕ_n . (○) $T=1015 \text{ K}$, Hurley and Bunch [4]; (■) $T=815 \text{ K}$, present study.

$Y_3Al_5O_{12}$ [3,4]. Mitchell and Youngman [3] attributed the absence of defect clusters to the large amount of interstitials (20) which are needed for the nucleation of a secondary defect cluster [3]. Rabier et al. [6] showed that possible Burgers vectors in the structure of $Y_3Al_5O_{12}$ are quite large and the cations can randomly occupy the octahedral, tetrahedral and dodecahedral sites when the cations are trivalent. This last feature makes recombination of the cation interstitials more possible than when the cations may occupy only one site.

4.2. Magnesium aluminate spinel

The observed volume changes of polycrystalline $MgAl_2O_4$ are compared with the results of other neutron studies in Fig. 4. $MgAl_2O_4$ was irradiated with neutrons in sodium-cooled reactors in the other studies. The large uncertainty in the swelling in the present study may be due to the fabrication technique as described in paragraph 2.1. This technique causes the pellets not to be completely cylindrical which makes them more difficult to measure with the micrometer. It must be noted that the isostatically pressed pellets ($Y_3Al_5O_{12}$ and Al_2O_3) are polished into a cylinder after the first sintering step. Their cylindrical shaped habit results into an error in the measurements of less than 0.3 vol.%.

Fig. 4 shows that neutron-irradiated spinel at a temperature of 660–815 K has negative swelling and at a temperature of 925–1100 K has positive swelling. The positive swelling is due to the creation of voids along grain boundaries [9]. In the present study, TEM samples show no sign of voids. The possibility of voids (and dislocation loops) is rate-limited by oxygen due to its larger activation energies for migration than Mg and Al. The activation energy of the migration of oxygen

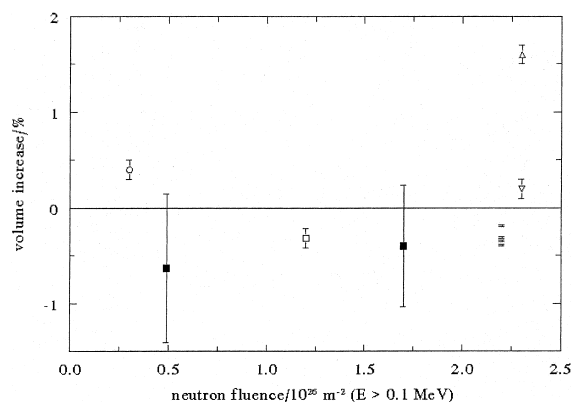


Fig. 4. The swelling of polycrystalline $MgAl_2O_4$ as a function of ϕ_n . (\square) $T=660$ K, Tucker et al. [7]; (\circ) $T=680$ K–815 K, Clinard et al. [8], only error bar is shown; (∇) $T=925$ K, (\triangle) $T=1015$ K, (\triangle) $T=1100$ K, Clinard et al. [9]; (\blacksquare) $T=815$ K, present study.

interstitial is larger than 4.0×10^{-19} J (2.5 eV) [10]. The oxygen interstitials (and cation interstitials) could therefore migrate to the grain boundaries at a temperature of 925–1100 K. A vacancy supersaturation had occurred which was high enough for void nucleation at temperatures of 925–1100 K. This is less favourable at a temperature of 815 K. A neutron irradiation study of spinel at 430 K to an amount of 30 dpa (ϕ_n is $2.1 \times 10^{26} \text{ m}^{-2}$, with $E > 0.2$ MeV) in a water-cooled reactor also showed positive swelling (0.8 ± 0.1 vol.%) because of “retention of point defects and small aggregates as a result of low mobility at this temperature” [11].

It is not yet clear why neutron-irradiated polycrystalline $MgAl_2O_4$ has a negative swelling at 660–815 K. The increased density may not be due to increased randomisation of the cations in the octahedral and tetrahedral sites, since synthetic spinel already contains a random distribution of the cations.

TEM results show almost no difference between un-irradiated TEM samples and irradiated ones, in the present study. The crystal structure of spinel shows that 75% of the cation sites are constitutional cation vacancies. Thus a large sink for the cation interstitials is present which may prevent them participating in clustering into stoichiometric interstitial loops.

The observation of almost no aggregated defects resolvable by TEM in neutron-irradiated polycrystalline spinel in the present study is in contrast with a previous neutron irradiation study of spinel at 800 K in which ‘dense arrays of interstitial dislocation loops’ were observed in every grain [7]. This study by Tucker et al. [7] did not show the damage rate (e.g. the fast neutron flux). This parameter is important for the *chance* of interstitial clustering or whether a cation interstitial has the time to recombine with a constitutional cation vacancy. Other features like grain size, impurities and gamma heating rate may also have an impact on the difference between the present study and the study by Tucker et al. [7].

The cause of the radial crack that is optically observed at each ϕ_n , is yet unclear. This crack may be due to thermal stresses in the pellet induced by gamma heating.

4.3. α -Alumina

The crystal structure of α - Al_2O_3 has 33% constitutional cation vacancies. This sink for aluminium interstitials may prevent aluminium to participate in interstitial clustering. However, the observation of a dense network of dislocation loops in the neutron-irradiated Al_2O_3 grains indicates that clustering of aluminium and oxygen interstitials in interstitial dislocation loops occurs.

Fig. 5 shows the volume changes in polycrystalline Al_2O_3 in comparison with other neutron studies at a temperature range of 660–1100 K. Al_2O_3 was irradiated

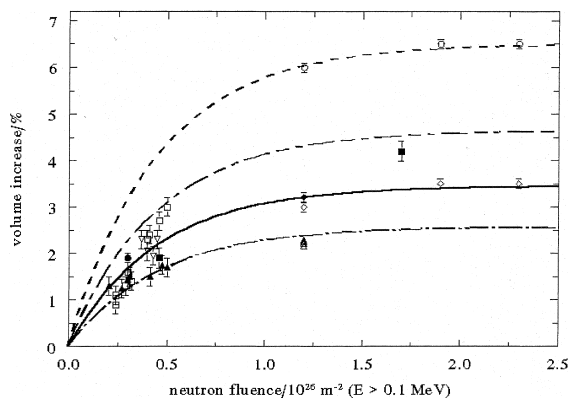


Fig. 5. The swelling of polycrystalline Al_2O_3 as a function of ϕ_n ; (\blacklozenge) $T=660$ K, Tucker et al. [7]; (\blacklozenge) $T=925$ K, (\bullet) $T=1015$ K, (\circ) $T=1100$ K, Clinard et al. [9]; (\triangle) $T=658$ K, Pells et al. [12], error bar unknown; (\blacktriangle) $T=650$ K, (∇) $T=875$ K, (\square) $T=1015$ K, Clinard et al. [13]; (\blacksquare) $T=815$ K, present study. The fittings curves Eq. (1) are: ($-\cdot-\cdot-$) $T=660$ K; ($-\cdot-$) $T=925$ K; ($-\cdot-\cdot-$) $T=1015$ K; ($\cdot\cdot\cdot$) $T=1100$ K.

with neutrons in sodium-cooled reactors in the other studies. For a sample of volume V , the swelling (ΔV) increases with increasing neutron fluence until a ϕ_n of $2 \times 10^{26} \text{ m}^{-2}$. The maximum of swelling (ΔV_{Max}) increases with irradiation temperature. Data points in the temperature region 660–1100 K were fitted. The calculation is carried out using the following equations:

$$100 \frac{\Delta V}{V} = 100 \frac{\Delta V_{\text{Max}}}{V} (1 - e^{-\phi_n/\Phi}), \quad (1)$$

$$100 \frac{\Delta V_{\text{Max}}}{V} = a + b \cdot e^{-h/T}. \quad (2)$$

The symbols in the equations are the flux exponential factor Φ : $0.45 \times 10^{26} \text{ m}^{-2}$, the constant a : 2.55, the pre-exponential factor b : 7517, and the exponential factor h : 8307 K. ϕ_n is given in m^{-2} and T in Kelvin.

The form of Eq. (1) is defined using the following considerations:

(1) The saturation of the swelling (at $\phi_n > 2 \times 10^{26} \text{ m}^{-2}$) is likely to be independent of the neutron irradiation temperature for all data points. The saturation can be well described by a negative exponential term. An explanation of this saturation is given after point 3).

(2) The swelling must be zero for $\phi_n = 0 \text{ m}^{-2}$; therefore the factor $(1 - e^{-\phi_n/\Phi})$ is appropriate;

(3) The crystal structure of $\alpha\text{-Al}_2\text{O}_3$ shows that aluminium and oxygen atoms are arranged in basal planes perpendicular to the c -axis. The number of neighbour sites is 6 in the basal plane and 2 in the c -axis. The distance between the neighbour atoms is 2.790 Å in the basal plane and 2.650 Å in the c -axis. There is therefore dissimilarity in diffusion of particles between the axes.

The extent of alignment of the voids (and dislocation loops) may increase exponentially with temperature since diffusion properties of solids are exponentially related to the reciprocal of the temperature. Therefore, the exponential relationship (2) may be assumed for the pre-exponential factor of Eq. (1). X-ray analysis of neutron-irradiated Al_2O_3 [9,14–16] showed a change in the lattice parameters after neutron irradiation which is due to alignment of dislocation loops or voids. This change in lattice parameter increased with irradiation temperature [9,14]. This confirms the hypothesis that anisotropic grain growth may depend on the different diffusional properties of the axes.

The exponential factor h (8307 K) may correspond to an activation energy of $1.15 \times 10^{-19} \text{ J}$ (0.72 eV). This value is low in comparison with the activation energy of anion and cation vacancy migration which is $2.8836 \times 10^{-19} \text{ J}$ (1.8 eV) [17]. However, diffusion of ions in dislocations (e.g. pipe diffusion) and grain boundaries may have an activation energy for migration which is 2–5 times lower than diffusion in the lattice [18]. A more detailed description of swelling can be made considering:

(1) the creation of (stoichiometric) interstitial and vacancy clusters;

(2) diffusion properties of clusters and point defects in the lattice, along grain boundaries, dislocations and pores;

(3) the impact of stress, created by anisotropic grain growth, on the dissimilarity in diffusion of particles between the axes;

(4) the influence of γ -radiation and impurities on the diffusion of particles.

However, a complete physical description of the swelling is beyond the scope of this paper.

The saturation swelling (see point 1) may be due to a steady-state of nucleation and dissolution of vacancies toward the void. The stable size of the void depends on temperature. In the study by Clinard et al. [5], the volume for each void increased about 16 times in the swelling saturation region (ϕ_n is $2.1 \times 10^{26} \text{ m}^{-2}$) in the temperature range from 925 to 1100 K. However, the concentration of voids in this neutron irradiation study, reported in Clinard et al. [9], decreased about 16 times in the same temperature range. Thus there should be no significant difference in swelling between 925 and 1100 K for each separate grain but more misfits in the grain boundaries occur due to increased anisotropic grain growth with increasing temperature.

The reduction for adhesion between the grains may be the reason that TEM results rarely show grain boundaries in neutron-irradiated polycrystalline Al_2O_3 in the present study since grains may preferably break at the grain boundaries during the crushing of the TEM samples. In Clinard et al. [9], separation at grain boundary was shown in neutron-irradiated polycrystalline Al_2O_3 at 1100 K, “presumably due to the necessity to

accommodate anisotropic swelling from adjacent grains”.

The equations match with the data of neutron studies in sodium-cooled reactors in Fig. 5, except for the study by Tucker et al. [7] and for very small neutron fluences. In the present study, the swelling of polycrystalline Al_2O_3 in a water-cooled reactor at 815 K is large in comparison with the swelling in a sodium-cooled reactor at a similar temperature.

5. Conclusion

TEM results reveal no differences between unirradiated $\text{Y}_3\text{Al}_5\text{O}_{12}$ samples and irradiated samples which are exposed to a neutron fluence of $1.7 \times 10^{26} \text{ m}^{-2}$ at a temperature of 815 K. TEM results of neutron-irradiated MgAl_2O_4 show separate dislocation loops in some grains but almost no defect aggregates are observed for a neutron fluence of $1.7 \times 10^{26} \text{ m}^{-2}$. The volume changes are smaller than 1% for both $\text{Y}_3\text{Al}_5\text{O}_{12}$ and MgAl_2O_4 . The negligible effect of neutron irradiation on these compounds makes them suitable inert matrix candidates for actinide fuels.

Al_2O_3 shows a relatively large volume change of 4.2% after irradiation. TEM results show a high density of dislocation loops in the grains at both neutron fluences of 0.46×10^{26} and $1.7 \times 10^{26} \text{ m}^{-2}$.

Acknowledgements

R. Belvroy, F. van den Berg, H. Buurveld, G. Dassel, W. Tams and, J.G. van Raaphorst of NRG are acknowledged for performing the pre- and post-irradiation examinations.

References

- [1] R.J.M. Konings, K. Bakker, J.G. Boshoven, R. Conrad, H. Hein, *J. Nucl. Mater.* 254 (1998) 135.
- [2] C. Kinoshita, K. Fukumoto, K. Fukuda, F.A. Garner, G.W. Hollenberg, *J. Nucl. Mater.* 219 (1995) 143.
- [3] T.E. Mitchell, R.A. Youngman, Proceedings of the Seventh International Conference on High Voltage Electron Microscopy Berkeley, 16–19 August 1983, p. 163, Lawrence Berkeley Laboratory report, LBL-16031.
- [4] G.F. Hurley, J.M. Bunch, *Am. Ceram. Soc. Bull.* 59 (1980) 456.
- [5] F.W. Clinard Jr., G.F. Hurley, R.A. Youngman, L.W. Hobbs, *J. Nucl. Mater.* 133&134 (1985) 701.
- [6] J. Rabier, P. Veyssière, J. Grilhé, *Phys. Stat. Sol.* 35 (1976) 259.
- [7] D.S. Tucker, T. Zocco, C.D. Kise, J.C. Kennedy, *J. Nucl. Mater.* 141–143 (1986) 401.
- [8] F.W. Clinard Jr., G.F. Hurley, L.W. Hobbs, D.L. Rohr, R.A. Youngman, *J. Nucl. Mater.* 122&123 (1984) 1386.
- [9] F.W. Clinard Jr., G.F. Hurley, L.W. Hobbs, *J. Nucl. Mater.* 108&109 (1982) 655.
- [10] W.A. Coghlan, F.W. Clinard Jr., N. Itoh, L.R. Greenwood, *J. Nucl. Mater.* 141–143 (1986) 382.
- [11] L.W. Hobbs, F.W. Clinard, S.J. Zinkle, R.C. Ewing, 216 (1994) 291.
- [12] G.P. Pells, S.N. Buckley, P. Agnew, A.J.E. Foreman, M.J. Murphy, S.A.B. Staunton-Lambert, Harwell Laboratory Report, AERE-R-13222, 1988.
- [13] F.W. Clinard, J.M. Bunch, W.A. Ranken, Los Alamos Report, LA-UR-75-1840, 1975.
- [14] R.H. Zee, W.Y. Wu, B.A. Chin, *J. Nucl. Mater.* 191–194 (1992) 571.
- [15] K. Tanimura, N. Itoh, F.W. Clinard, *J. Nucl. Mater.* 150 (1987) 182.
- [16] B.S. Hickman, D.G. Walker, *J. Nucl. Mater.* 18 (1966) 197.
- [17] W.D. Kingery, *Advances in Ceramics*, vol. 10, American Ceramic Society, 1984, p. 72.
- [18] J.P. Poirier, *Creep of Crystals*, Cambridge University, Cambridge, 1990, p. 50.